ORIGINAL ARTICLE

Natural controls validation for handling elevated fluoride concentrations in extraction activated Tóthian groundwater flow systems: San Luis Potosí, Mexico

Antonio Cardona[1] · Andre Banning[2] · José Joel Carrillo-Rivera[3] · Alfredo Aguillón-Robles[4] · Thomas R. Rüde[5] · Jorge Aceves de Alba[1]

Abstract

Fluoride concentration in groundwater supply above the guideline value of 1.5 mg/L is a health hazard for the population living in two thirds of the Mexican territory. Enhanced groundwater extraction in the city of San Luis Potosí (SLP), Mexico, led to a substantial territorial increase in water with high fluoride (F^-) which originates from thermal water–rock interaction with regional rhyolites. Previous knowledge of the Tóthian groundwater flow systems around SLP City and their F^- concentrations from 1987 data provided an insight into natural F^- controls for the construction and operation of boreholes. During the period 1987–2007, the number of new boreholes increased as well as the relocation of boreholes whose production diminished. Overall estimated extraction augmented from 2.6 to 4.1 m^3/s. Results obtained for 2007 suggest that F^- controls defined for 1987 data (e.g., variable portions of F^--rich deep thermal water in borehole yields) are also valid in newly constructed boreholes. Water authority actions related to groundwater extraction lack consideration of proposed F^- controls, so constructed boreholes progressively tapping the high F^- groundwater flow system resulted in a 85% increase in the F^- affected territory (> 2 mg/L) between 1987 and 2007. Reduction in F^- extraction following the proposed natural control mechanisms (e.g., fluorite precipitation) was also confirmed. Applying geochemical and mineralogical analysis, rhyolites surrounding the SLP graben basin and contributing to its volcano-clastic sedimentary filling were identified as the primary F^- source for elevated concentrations in groundwater of the area under investigation.

Keywords Hydrochemistry · Fluorosis · Arid regions · Volcanic aquifer · Groundwater management · Mexico

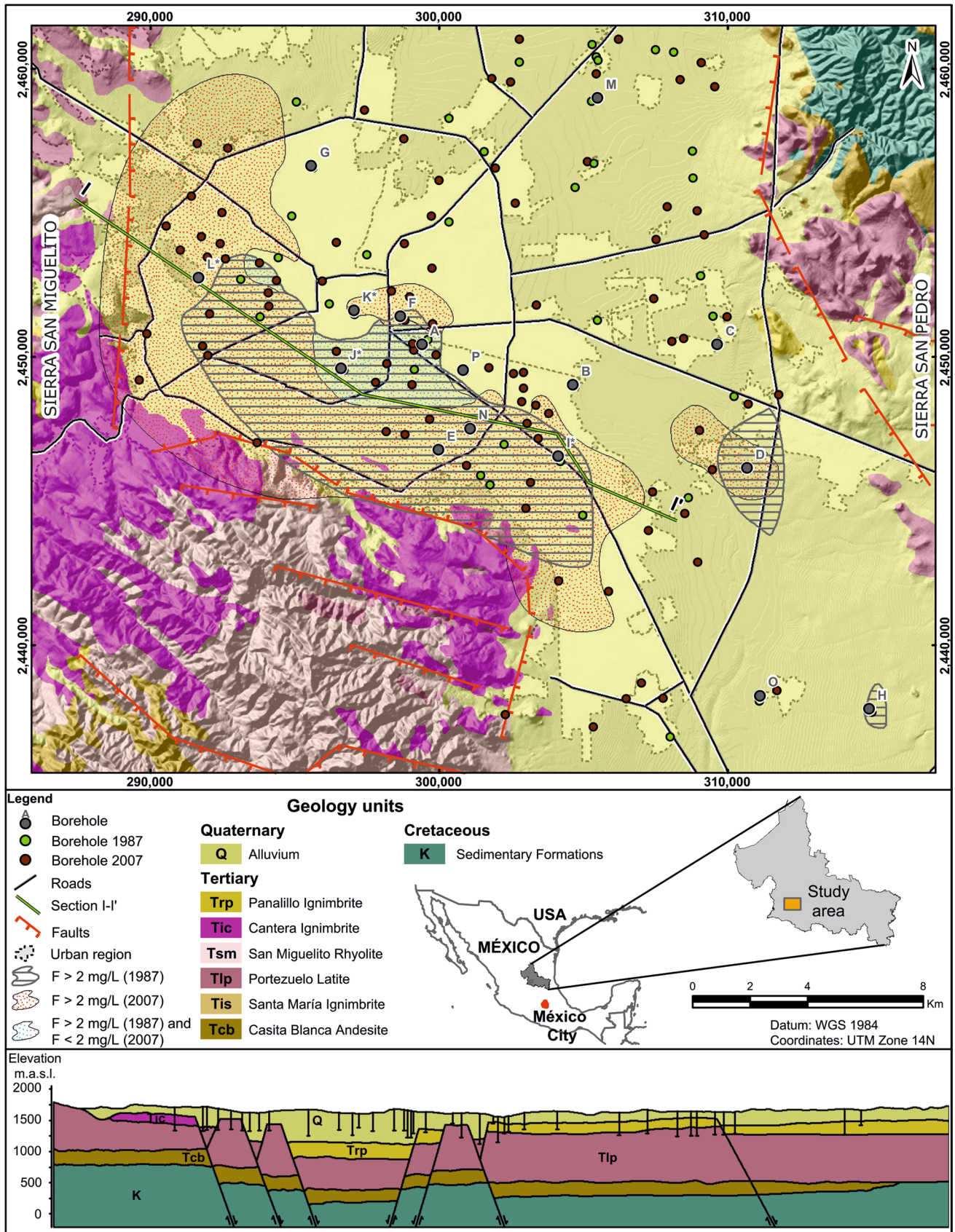✉ Andre Banning
andre.banning@rub.de

1 Earth Sciences, Universidad Autónoma de San Luis Potosí, Dr. Manuel Nava No. 8, 78290 San Luis Potosí, Mexico

2 Hydrogeology Department, Ruhr-Universität Bochum, Universitätsstr. 150, 44801 Bochum, Germany

3 Institute of Geography, Universidad Nacional Autónoma de México, C.U., Coyoacán, 04510 Mexico City, Mexico

4 Institute of Geology, Universidad Autónoma de San Luis Potosí, Dr. Manuel Nava No. 5, 78240 San Luis Potosí, Mexico

5 Institute of Hydrogeology, RWTH Aachen University, Lochnerstr. 4-20, 52064 Aachen, Germany

Introduction

Importance of fluoride management

Groundwater is the major source of potable water supply in arid and semiarid regions. However, its availability may be threatened not only by the introduction of contaminants through human activities but also by natural processes (McArthur et al. 2012; Nicolli et al. 2012; Jia et al. 2014; Edmunds et al. 2015; Banning and Rüde 2015). The contribution of some minor and trace elements (e.g., fluoride, iron, arsenic, uranium, lead, and cadmium) that change the quality of extracted groundwater is a substantial health hazard in many groundwater regions worldwide (e.g., Edmunds and Smedley 1996; Fendorf et al. 2010; Guo et al. 2014; Jia et al. 2014, 2017; Bjørklund et al. 2017). Recently, the impact of trace elements in the water supply of Mexico has started to be given consideration in groundwater management.

Legend

- Borehole
- Borehole 1987
- Borehole 2007
- Roads
- Section I-I'
- Faults
- Urban region
- F > 2 mg/L (1987)
- F > 2 mg/L (2007)
- F > 2 mg/L (1987) and F < 2 mg/L (2007)

Geology units

Quaternary
- **Q** Alluvium

Tertiary
- **Trp** Panalillo Ignimbrite
- **Tic** Cantera Ignimbrite
- **Tsm** San Miguelito Rhyolite
- **Tlp** Portezuelo Latite
- **Tis** Santa María Ignimbrite
- **Tcb** Casita Blanca Andesite

Cretaceous
- **K** Sedimentary Formations

Study area

Datum: WGS 1984
Coordinates: UTM Zone 14N

◀**Fig. 1** Morphologic–geological map of the study area (including territories with high groundwater F⁻ concentrations 1987 and 2007, and location of the sampled boreholes in the SLP graben basin), location of the study area in Mexico, and geological cross section I–I′ (bottom; including the location of sampled boreholes along it). *Sources*: simplified geological and structural map modified after Labarthe-Hernández et al. (1982) and Tristán-González (1986); digital elevation model from INEGI (2013)

Carrillo-Rivera et al. (2002) proposed feasible natural F⁻ management controls at borehole site without the need of a water treatment plant. These management approaches might be applied elsewhere as F⁻ is a common natural constituent that threatens groundwater supply in both industrialized and developing countries (e.g., Lucas 1988; Gaciri and Davies 1993; Valenzuela-Vásquez et al. 2006; Amini et al. 2008; Nicolli et al. 2012; Guo et al. 2012; Navarro et al. 2017; Raju 2017). In the semiarid eastern part of the Sierra Madre Occidental alone, at least some 15% of the total Mexican population (estimated to be in excess of 110 million people), are supplied with regional F⁻-rich groundwater.

Study area

The investigation area is located around San Luis Potosí (SLP) City, capital of the homonymous state, in the semi-arid north-central part of Mexico (Fig. 1). It hosts one of the conurbations of the country with the highest population growing rate (broadly 5–7% p.a.), and presently has around one million inhabitants.

The study area is part of one of the several closed basins existing in the north-central part of Mexico. The steep surrounding mountain ranges of Sierra de San Miguelito (SSM, west of SLP) and Sierra de San Pedro (SSP, east of SLP) consist of Tertiary felsic volcanic and Cretaceous calcareous rocks, respectively (Fig. 1). These sierras have an elevation exceeding 2300 m a.m.s.l. and slope toward the plane of the drainage basin which has an altitude of about 1900 m a.m.s.l. The mean annual air temperature is around 17.5 °C, while the summer mean temperature is around 21 °C.

The San Luis Potosí Volcanic Field (SLPVF) is located between the morphotectonic province of Sierra Madre Oriental, and the volcanic province of Sierra Madre Occidental (Guzmán and De Cserna 1963), in the southern part of the Mesa Central. The main local geological features are associated with a thick (> 1500 m) sequence of extrusive tertiary volcanic rocks and alluvial materials, covering a Cretaceous limestone and calcareous mudstone sequence outcropping in folded NW–SE-striking structures in SSP (Fig. 1, cross section); suchlike features are typical for a number of similar basins in the Sierra Madre Occidental (400 km wide and 1500 km long, hosting volcanic rocks with a total thickness of 2–3 km) and other regions of northwestern Mexico and the southwestern USA. The Tertiary volcanic units relevant

for this study were generated in several stages and are briefly presented in the following paragraph, according to the volcano-stratigraphy developed by Labarthe-Hernández et al. (1982; cf. Fig. 1).

The emplacement of the SLPVF began with the *Casita Blanca Andesite* which is composed of basaltic to andesitic lava flows of porphyric texture with ~ 5 vol.% of biotite and plagioclase phenocrystals; ages obtained for this unit are between 43.7 and 36.5 Ma (Tristán-González et al. 2009). The subsequent *Santa María Ignimbrite* yields welded ash-flow tuffs with 30–40 vol.% of mainly quartz and sanidine phenocrystals and collapsed pumice (Tristán-González et al. 2006, 2009). The *Portezuelo Latite*, generated around 30.6 Ma, consists of different lava flows with porphyric texture (30 vol.% of sanidine, albite, and quartz phenocrystals). It overlies some Mesozoic marine formations with discordant contact and is stratigraphically followed by the *Panalillo Ignimbrite* (Tristán-González 1986). The latter unit is composed of two members with the inferior member consisting of pyroclastic flows filling small tectonic structures and the superior one of co-ignimbrite and welded ignimbrite; their age is between 26.8 and 28.0 Ma (Tristán-González et al. 2009). The *San Miguelito Rhyolite* was named after the outcrop of the lava flows in the Sierra de San Miguelito. This widespread unit is composed of highly viscous, topaz-bearing lava flows that formed dome structures showing flow foliation, shrinkage fractures and tephra surges similar to structures reported from the USA by Christiansen et al. (1983). This rock has 5–20 vol.% of phenocrystals of quartz and feldspar in the devitrified matrix (Aguillón-Robles et al. 1994; Tristán-González et al. 2009). The *Cantera Ignimbrite* was described as a violet to gray colored rock with 5–10 vol.% of phenocrystals (quartz and sanidine) and uncollapsed pumice. It is associated with the main volcanic event of the Sierra de San Miguelito. The *El Zapote Rhyolite* (not sampled for this study) represents the latest volcanic event of the Sierra de San Miguelito and is composed of gray colored lava flows with ~ 30 vol.% of phenocrystals (quartz, sanidine) and an isotopic age of 27.0 Ma (Nieto-Samaniego et al. 1996). Overall, the studied volcanic rocks are geochemically well differentiated (felsic to intermediate).

Expansive structures (mainly normal faults) bound a regional horst and graben structure and were used as conduits for volcanism (Tristán-González 1986). Based on geochemical variations, Orozco-Esquivel et al. (2002) divided the described succession into a lower and an upper volcanic sequence. The younger (upper) one consists of mainly rhyolitic lavas that contain topaz and are enriched in F and incompatible lithophile elements. This subdivision was adopted for geochemical interpretations in the present study (cf. "Geochemical and mineralogical characterization of the fluoride source" section). The allocation of the sampled lithologies for the two sequences can be found in Table 1.

Table 1 Selected geochemical data of volcanic rocks from the study area and its vicinity (own analyses and data from Orozco-Esquivel et al. 2002 and Rodríguez-Ríos 1997)

Stratigraphy	Sample	Si wt.%	Al	Fe	Ca	Mg	Na	K	F μg g^{-1}	Rb	Sr	Zr	Nb	Ba	La	Eu	Yb	Ta	Th
Upper sequence																			
IC	M-5	35.7	6.6	0.8	0.0	0.1	2.0	4.4	608	272	32	147	30	203	27.6	0.5	7.3	2.0	25
	M-6	35.5	6.7	0.9	0.3	0.0	2.4	4.2	595	269	46	166	29	318	57.6	0.5	5.3	1.9	39
IP	M-8	35.5	6.9	1.1	0.1	0.0	2.5	4.1	116	251	9	300	53	62	61.9	0.3	8.0	3.1	40
SSM	M-7	35.9	6.5	1.2	0.2	0.0	2.2	4.1	2651	594	7	139	44	64	25.5	0.1	8.5	4.2	79
	M-9	35.3	6.8	1.1	0.1	0.0	2.4	4.0	1032	375	18	151	32	258	32.3	0.2	6.3	2.8	46
	CG/95/3	31.9	7.4	2.4	0.7	0.0	1.2	4.8	2100	484	6	137	34	17	37.1	0.1	4.5	5.1	55
	CG/95/4	31.8	7.3	2.8	0.6	0.1	1.1	4.6	1900	499	8	135	36	43	24.7	0.1	5.4	5.3	37
	CG/95/5	32.1	7.2	2.8	0.6	0.1	1.1	4.4	3500	479	7	134	32	22	67.9	0.1	13.2	4.8	62
	CG/95/7	36.4	6.1	1.0	0.3	0.0	1.7	4.7	1700	399	9	141	25	34	20.8	0.1	3.6	3.4	38
	CG/95/9	34.5	6.8	1.8	0.2	0.0	1.5	4.8	2400	75	10	127	33	62	11.7	0.1	5.7	5.0	46
	CG/95/49	34.2	6.4	2.4	0.2	0.0	1.2	5.6	2500	471	12	130	34	62	13.3	0.1	3.3	5.0	45
	CS/95/10	34.7	6.5	1.6	0.6	0.0	1.4	4.8	600	262	27	160	19	276	68.4	0.3	5.1	2.2	34
	CS/95/11	35.1	6.9	1.8	0.5	0.0	1.9	4.6	1000	265	17	124	20	101	50.2	0.2	5.6	2.5	33
	CS/95/12	35.3	6.7	1.4	0.5	0.0	1.9	4.0	800	275	27	125	21	625	46.5	0.2	4.9	2.5	33
	CS/95/14	35.6	6.2	1.6	0.6	0.0	1.9	4.2	2500	432	8	131	29	77	13.3	0.1	6.0	4.2	36
RS	DS/96/2	36.4	6.0	1.0	0.2	0.4	1.4	4.1	540	316	100	248	17	705	41.0	0.8	2.0	2.1	20
	DS/96/3	36.2	6.0	1.0	0.3	0.5	2.0	4.0	1600	317	100	266	19	747	58.8	1.1	3.3	2.3	21
	DS/95/28	36.2	5.9	0.9	0.2	0.4	1.9	4.0	1200	248	100	228	17	611	47.6	1.1	3.5	1.8	21
RC	DS/95/22	35.6	6.4	1.3	0.1	0.0	2.1	3.9	410	290	32	213	21	283	53.6	0.5	5.9	2.7	28
	DS/95/45	33.3	7.1	3.3	1.2	0.0	2.1	4.2	170	221	24	387	37	341	100	1.0	7.3	3.0	24
	DS/96/1	33.6	7.0	2.5	1.6	0.1	2.2	4.2	340	254	112	275	20	851	74.0	1.1	3.0	2.1	22
R	RIO-16	35.5	6.9	1.0	0.4	0.1	2.5	4.5	7603	581	6	125	42	50	75.8	0.2	19.2	6.2	85
	RIO-12	35.6	7.0	1.0	0.3	0.1	2.1	4.6	1463	407	9	113	19	28	17.9	0.1	5.5	3.9	36
	RIO-9	35.9	6.8	1.1	0.2	0.1	2.0	4.1	1289	307	9	86	24	49	10.0	0.1	6.2	3.2	30
	RIO-44	35.9	6.7	1.0	0.2	0.1	2.5	4.0	2840	601	7	143	30	89	24.3	0.1	5.0	5.5	57
	RIO-41	36.3	6.5	0.9	0.3	0.1	1.9	4.2	1296	359	8	144	23	20	21.7	0.1	5.2	3.3	33
	RIO-46	36.5	6.2	0.8	0.4	0.1	1.9	4.2	1149	330	9	112	18	49	35.3	0.1	7.2	2.9	28
	RIO-43	36.6	6.2	0.9	0.4	0.1	1.9	4.2	1039	322	13	145	17	70	28.7	0.2	6.0	2.7	32
	RIO-7	36.3	6.6	1.0	0.1	0.1	1.5	4.0	356	186	20	113	16	137	19.6	0.3	3.9	1.7	16
Ø RU		35.1	6.6	1.5	0.4	0.1	1.8	4.3	1691	359	27	162	26	218	39.3	0.3	6.0	3.5	38
Ø RSM		34.4	6.7	1.8	0.4	0.0	1.6	4.6	1890	384	12	136	29	136	34.3	0.1	6.0	3.9	45
Lower sequence																			
ACB	M-1	25.5	8.7	6.2	5.4	2.5	2.5	1.5	1005	47	572	322	14	684	39.0	1.9	2.4	0.7	6
LP	M-4	31.4	6.7	3.8	2.9	0.2	2.0	3.7	592	199	205	380	24	2371	77.7	1.9	6.3	1.9	18
ISM	M-2	35.4	5.9	2.4	0.7	0.1	1.8	4.2	358	189	98	234	22	1346	50.7	1.1	3.5	1.3	24
R	RIO-45	33.3	7.1	3.3	1.2	0.2	2.1	4.2	1082	189	141	501	18	1340	53.6	1.7	4.5	1.8	17
	RIO-29	33.6	7.0	2.5	1.6	0.2	2.2	4.2	1336	159	129	457	16	1630	59.0	1.6	4.8	1.9	16
	RIO-22	34.7	6.5	1.6	0.6	0.3	1.4	4.8	322	193	62	278	13	1300	61.2	1.1	4.6	1.8	18
	RIO-18	35.1	6.9	1.8	0.5	0.2	1.9	4.6	250	170	91	277	13	1480	61.6	1.3	4.4	1.7	16
	RIO-47	35.3	6.7	1.4	0.5	0.1	1.9	4.0	207	181	78	304	14	1410	77.8	1.4	5.7	1.5	18
	RIO-24	35.6	6.2	1.6	0.6	0.1	1.9	4.2	489	155	90	250	15	1360	53.5	1.2	3.9	1.8	19
Ø RL		34.6	6.7	2.0	0.8	0.4	1.9	4.3	614	174	98	344	14	1420	61.1	1.4	4.7	1.8	17
Ø RU/Ø RL		1.01	0.98	0.75	0.51	0.25	0.95	1.00	2.75	2.06	0.27	0.47	1.76	0.15	0.64	0.23	1.28	1.99	2.21
Ø RSM/Ø RL		0.99	1.00	0.90	0.50	0.00	0.85	1.05	3.08	2.20	0.13	0.40	2.01	0.10	0.56	0.10	1.29	2.24	2.62

ACB Casita Blanca Andesite, *LP* Portezuelo Latite, *ISM* Santa María Ignimbrite, *IC* Cantera Ignimbrite, *IP* Panalillo Ignimbrite, *RSM* San Miguelito Rhyolite, *RS* Santana Rhyolite, *RC* Carbonera Rhyolite, *R* rhyolites from different domes and flows, *RL* Lower sequence rhyolites, *RU* Upper sequence rhyolites

A clastic sequence of debris flow sediments containing volcanic material derived from the weathering of the surrounding volcanic rocks syn-tectonically filled the graben structure as basin-fill sediments. Calcareous material resulting from erosion of Cretaceous rocks in Sierra San Pedro also contributed to these sediments and is interbedded with the pyroclastic material; the total filling is referred to as Tertiary Granular Undifferentiated (TGU). Cardona (2007) used information from borehole logging, resistivity surveys, and lithology samples to determine the general granulometric distribution and thickness of the basin filling. Depending on the intra-graben position, the granulometric distribution varies from alluvial fan deposits to playa sediments in the lowest topographical part of the graben structure. Depth to the Tertiary fractured volcanic rocks beneath the basin-fill sediments is about 250–300 m on average with highest thicknesses of about 450–500 m in the northeastern region of SLP City.

Within the SLP City plain, two main hydrogeological units—(I) shallow and (II) deep aquifer—are vertically separated by a fine-grained layer with low hydraulic conductivity (ca. 10^{-11} m/s). The shallow alluvial aquifer unit is unconfined, while the deep aquifer unit is confined below the mentioned fine-grained layer and unconfined elsewhere, being heterogeneous and anisotropic in both fractured (volcanic rocks) and granular (TGU) material. Cretaceous carbonate rocks represent the lower flow boundary.

Information presented by Carrillo-Rivera et al. (1996, 2002, 2007) and Cardona and Carrillo-Rivera (2006) indicate the presence of two flow systems sensu Tóth (1998) in the deep aquifer unit: (IIa) a deep regional flow system represented by thermal water (35–40 °C at borehole head); elevated B, F, Na, and Li concentrations indicate interaction with fractured volcanic rocks, and (IIb) an intermediate shallow flow system with a temperature of 23–28 °C and low concentrations of B, F, Na, and Li, indicating interaction with the basin-fill sediments. Both systems are ^{3}H free. Absolute age determinations using ^{14}C indicate that actually extracted groundwater from the regional system is around 5000–6000 years old, while the intermediate system water shows ages of 2000–3000 years. Intensive water extraction was applied to the top of the deep aquifer unit to supply the growing city for the 1977–2007 period. This resulted in considerable groundwater table drawdown (ranging from 90 to 25 m) in deep (100–450 m below ground surface) boreholes following from an increase in total annual extraction from 1.9 to 4.1 m^3/s in the same period of time. As a consequence, old regional flow groundwater started ascending to the production boreholes depth.

Fluoride situation in SLP

Dental fluorosis has been increasingly reported from the inhabitants of the city of SLP (Carrillo-Rivera et al. 2002) and recognized as the result of high exposure to naturally occurring F$^-$ in the drinking water supply, a connection also observed in other parts of Mexico (e.g., García-Pérez et al. 2013). This is causing some degree of dental fluorosis in 84% of the inhabitants between 6 and 30 years of age; 34% of the 11–13-year-old children showed severe fluorosis (Medellín-Milán et al. 1993; Grimaldo et al. 1995). Severe dental fluorosis was observed in children only, and senior citizens lack significant effects (Sarabia 1989) suggesting the former have been in contact with comparatively higher F$^-$ concentrations in the water supply than the latter users.

Tapped groundwater in 1987 for SLP city comprised various proportions of the aforementioned shallow intermediate and the deep regional flow systems (Carrillo-Rivera et al. 2002). Mixing of these flows takes place depending on extraction regime, local contrast in hydraulic characteristics, and borehole construction, depth, design, and operation. Maximum F$^-$ concentrations found in 1987 (3.7 mg/L) were argued to become higher still, in time and space, should the input of regional F$^-$-rich flow to the extraction boreholes be further enhanced. The worst-case scenario would be the extraction of 100% of the deep regional flow component. It was suggested that by controlling the extraction borehole-head water temperature at 28–30 °C, an extracted raw water mixture with F$^-$ concentrations close to the maximum drinking water standard of 1.5 mg/L could be obtained (Carrillo-Rivera et al. 2002).

Historical chemical analyses of regional flow groundwater (Stretta and Del Arenal 1960) show remarkable temporal constancy in major ion hydrochemical composition. Field groundwater temperature measurements exhibit a linear relationship to F$^-$ concentrations which permits an indirect estimation for the F$^-$ concentration in extracted groundwater. Extraction rates increased from ≈ 0.6 m^3/s in the 1960s to ≈ 2.6 m^3/s in 1987, thereby inducing vertical F$^-$-rich water flow into boreholes (in this paper understood as all ground perforations with pumping equipment for the extraction of water serving for public supply) located in the center of the SLP catchment.

Assessing the situation in 1987, regionalization of F$^-$ concentrations in 52 groundwater samples from boreholes distributed in the territories as represented in Fig. 1 produced a surface area affected by high F$^-$ (> 2 mg/L) of about 73 km^2. The contour map represented by the 2 mg/L F$^-$ isoline was delineated using linear kriging without any data transformation (model range: 7483 m). The goodness of fit for the gridding method was calculated using residuals and the coefficient of multiple determination (R^2). Results for 1987 data indicate a R^2 value of 0.996, showing that in

this case linear kriging is a suitable method as compared with, e.g., polynomial regression ($R^2 = 0.401$). The high F^- (> 2 mg/L) surface area (135 km^2) determined for 2007 (107 groundwater samples) was delineated with the same gridding method. The higher sampling density allowed a model range of 4246 m, producing a R^2 value of 0.987. Comparison of F^- concentration values for the eastern, southern, and northeastern regions of the study area show no major evolution in the 1987–2007 period with most concentrations below the drinking water standard of 1.5 mg/L F^- (exceptions: territories associated with the boreholes D and H; Fig. 1). Consequently, further increase in groundwater extraction enhanced the surface area affected by high F^- (> 2 mg/L) inflow from 73 km^2 in 1987 to 135 km^2 in 2007 (i.e., + 85%; Fig. 1).

At present, the estimated withdrawal is ≈ 4.1 m^3/s, additional boreholes are mainly tapping the regional system at the foot of the felsic volcanic SSM to the west of the catchment. Additional F^- attenuation methods in extraction boreholes should consider the hydrogeological and geochemical control mechanisms of F^- as well as the borehole construction design to regulate the percentage of different groundwater flows supplying an extraction borehole. The objectives of this study are to characterize the primary F^- source, to evaluate natural F^- control under observed increased groundwater extraction in the SLP catchment and to reassess F^- attenuation measures as proposed under 1987 conditions.

Materials and methods

Water sampling and analyses

Standard water-sampling procedures included detailed field measurements of temperature, pH, Eh, dissolved O$_2$, and electrical conductivity (APHA-AWWA-WPCF 1989). An in-line flow cell at a by-pass of the standpipe was used to ensure exclusion of atmospheric interference and to improve measurement stability. Two filtered (0.45 μm) samples were taken at each site in acid-washed, well-rinsed low-density polyethylene bottles. One sample for major cation and trace element determination was acidified with high-purity HNO$_3$, producing a pH of about 2, sufficient to stabilize trace metals. One filtered, unacidified sample was collected for anion analysis. Alkalinity was obtained through standard volumetric Gran titration method using H$_2$SO$_4$ and a digital titration device. All used equipment was calibrated in situ. Water samples were kept at 4 °C before hydrochemical analysis. Chemical solutions used during field determinations were subject to quality control. All reported values have ionic balance errors within 5%, except 5 out of 140 samples which show errors below 10%. A complete suite of major (HCO$_3^-$, Cl$^-$, SO$_4^{2-}$, Ca^{2+}, Na$^+$, Mg^{2+}) and minor (NO$_3^-$, K$^+$, F$^-$)

ions as well as some trace element (Li, Sr, Fe, Mn) analyses were conducted, although for this investigation, only Li (atomic adsorption spectroscopy) and F (ion selective electrode) were considered for the interpretation of hydrochemical data. Water analyses were carried out at the Soil and Water Chemical Laboratory of the Engineering Faculty of the UASLP.

Rock sampling and analyses

Sampling of the volcanic rocks was done considering the stratigraphic volcanic sequence determined by Labarthe-Hernández et al. (1982), six out of the eight most representative volcanic units were sampled (8 samples) in different locations. In addition to own sampling and analysis, volcanic rock chemical data were taken from previous studies in the area (Orozco-Esquivel et al. 2002; Rodríguez-Ríos 1997) to extent the geochemical database to a total of 38 samples (1 andesite, 1 latite, 4 rhyolitic ignimbrite, 32 rhyolite samples) with a strong focus on rhyolites accounting for the dominance of this rock type in the study area. Whole-rock samples were analyzed for major elements using a Siemens SRS 3000 X-ray sequential spectrometer. The determination of trace elements was done by ICP-MS (Perkin Elmer ELAN 9000).

Three thin sections were produced from rhyolite samples (San Miguelito Rhyolite) of different alteration grades and studied under the microscope (Olympus IX70) using transmitted light and an ultraviolet lamp for the identification of F-bearing minor mineral phases. Aliquots of those three rhyolites were ground to powder grain size (McCrone corundum mill) and analyzed for their mineralogical composition using a Bruker AXS D8 Advance X-ray diffractometer (CuKα radiation; operational adjustments: 40 kV, 40 mA, $2\theta = 2°–92°$). The proportion of amorphous glassy material in the samples was estimated by adding an internal anatase standard (10 wt.% of total sample size).

Processing of analytical information

Available data on the physical and hydrochemical behavior of groundwater when flowing through different lithologies of the SLP region were interpreted based on the flow system theory (Tóth 1998) from where the hierarchy of different flow systems (local, intermediate and regional) have been defined with the combined use of additional geographical data (i.e., geomorphology, soil, and vegetation) suggesting the existence of recharge, transit, or discharge conditions. The conceptual contrasting biophysical differences, among others, of the different hierarchical flow systems assembled by Tóth (1998) allow to propose—above basic groundwater flow—systems that move individually under natural conditions. This characterization

Results and discussion

Geochemical and mineralogical characterization of the fluoride source

Geochemical data obtained from own analyses and previous studies (Orozco-Esquivel et al. 2002; Rodríguez-Ríos 1997) are presented in Table 1. Separation between Lower and Upper volcanic sequence was adopted as suggested by Orozco-Esquivel et al. (2002).

Major ion contents in rhyolites from both sequences are relatively stable, and average values are very similar (Table 1) with the exception of calcium which is depleted in the Upper sequence, compared to the Lower one. With an average content of nearly 1700 µg g^{-1}, F in Upper sequence rhyolites is enriched by a factor of 2.75 compared to Lower sequence rhyolites. This trend is even more pronounced in rhyolites from the Sierra San Miguelito (Ø nearly 1900 µg g^{-1} F; enrichment factor 3.08). For comparison, average F content in acid igneous rocks is 800–1000 µg g^{-1} (Lucas 1988). Fluorine enrichment in the Upper sequence occurs together with some incompatible large ion lithophile elements (LILE: Rb, Cs, Heavy REE, U, Th, Pb) and high-field-strength elements (HFSE: Nb, Ta) as shown by enrichment factors in Table 1 and correlation coefficients with F in Fig. 2d. On the contrary, feldspar-compatible elements (Ba, Sr, Eu), Zr, and Light REE are depleted in the Upper sequence. Both observations suggest F being hosted in late magmatic mineral phases or the matrix. These findings are in good agreement with the results of Orozco-Esquivel et al. (2002), indicating the regional rhyolites' geochemical

has proved to be applicable in the study area (Carrillo-Rivera et al. 2002, 2007). Under natural conditions, local flows have the shortest travel depth and distance, and contain groundwater with temperature closest to that of the recharge environment; therefore, this sub-recent water has comparatively low pH and total dissolved solids (TDS); its dissolved oxygen (DO) concentration is high. In contrast, the regional flow will travel the deepest and longest paths, achieving a water temperature and TDS as functions of depth and distance of travel. The pH of the water will increase, and its DO will decrease; it represents the oldest water in the system. An intermediate flow system can be developed between local and regional systems. In the study area, local flows are ephemeral showing their presence only during the rainy season; therefore, the next flow in the hierarchical position is the one of intermediate nature. Regional flow has been shown to be characterized by the highest temperature, Li and F$^-$ concentrations, due to its deepest traveling path and nature of the hosting felsic rock units, whereas intermediate flow has lower temperature as well as lesser Li and F$^-$ concentrations (Carrillo-Rivera et al. 2002). Using the hydrogeochemical modeling software Phreeqc (Parkhurst et al. 1980) allowed for the evaluation of water–mineral equilibria and mixtures between the identified flows.

Statistical analysis of the geochemistry dataset was conducted using the software SPSS Statistics 17.0. Quantification calculations of mineral phases after XRD determinations were conducted applying Rietveld analysis with the software BGMN, version 4.2.3.

Fig. 2 Fluorine correlation with other elements in studied volcanic rocks; **a** F-Th scatter plot, **b** F-Ca scatter plot, **c** F–Al scatter plot, **d** Pearson correlation coefficients F-[element] for all rhyolite samples, lines indicating distinct positive ($R^2 \geq 0.3$) and negative ($R^2 \leq -0.3$) correlation
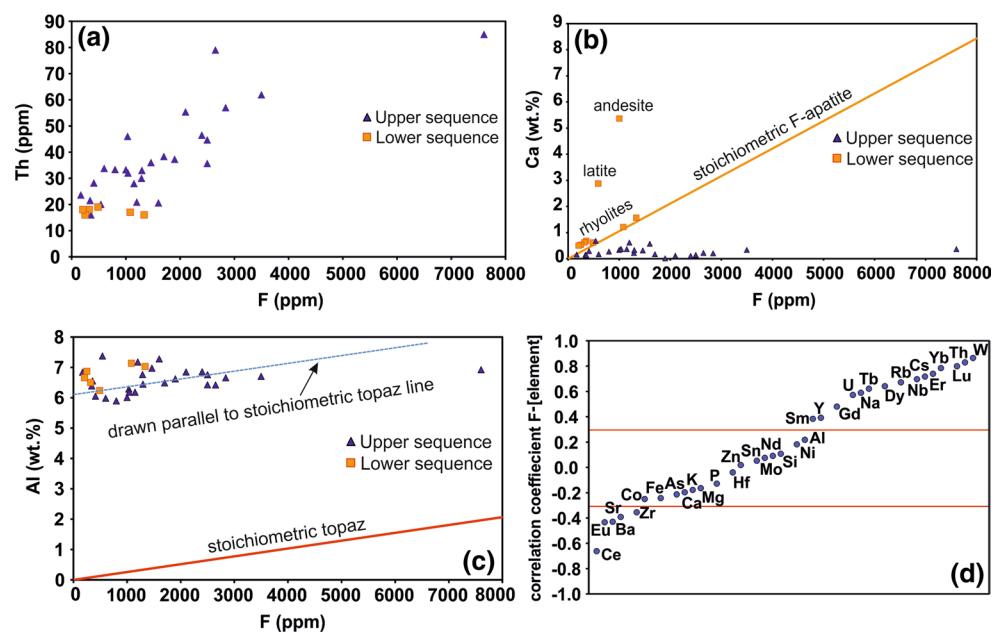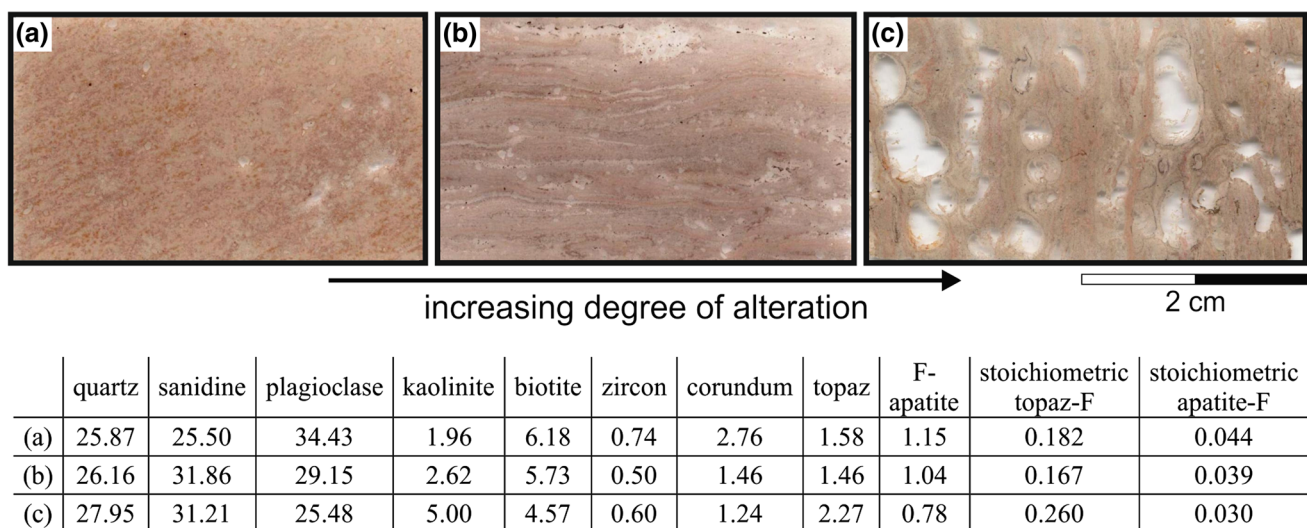
similarity to rhyolites from the western USA (Christiansen et al. 1983). This underlines the incompatible behavior of F and thus its tendency to be concentrated in the melt fraction during magmatic differentiation (e.g., Stecher 1998). Similar to F behavior, all mentioned enrichment and depletion trends of other elements are even more distinct when only Sierra San Miguelito rhyolites are taken into account (Table 1). Figure 2a–c illustrates F scatter plots versus different elements, with samples being differentiated between Upper and Lower volcanic sequence.

As an example for fluorine enrichment and occurrence together with incompatible elements, Fig. 2a shows a positive correlation ($R^2 = 0.69$) between F and Th in the Upper sequence, while no relation is observable in Lower sequence rhyolites. Figure 2b contains the stoichiometric F/Ca ratio of fluorapatite $Ca_5(PO_4)_3F$ with Lower sequence rhyolites closely ($R^2 = 0.98$) following this line (andesite and latite represent outliers with substantial excess Ca), while Upper sequence rhyolites developed differently, acquiring excess F. This suggests that fluorapatite controls the F budget of the Lower sequence rhyolites, while it is of lesser importance for the Upper sequence. The stoichiometric F–Al ratio of topaz $Al_2(SiO_4)F_{1.1}(OH)_{0.9}$ was implemented in Fig. 2c to evaluate the importance of this mineral phase for F distribution. In this diagram, Upper sequence rhyolites scatter subparallely to the topaz line (with large excess of Al caused by feldspar presence). This indicates F being at least partly bound in topaz, especially in the Upper sequence as reported by Orozco-Esquivel et al. (2002).

Quantitative X-ray diffraction results obtained by Rietveld analysis are presented in Fig. 3. Sample (a) represents an unweathered rhyolite, while (c) is a more altered sample [with (b) being intermediate between (a) and (c)]

as concluded from observation of rather grayish color and decreasing consolidation of the latter. This is supported by mineralogical results showing a decrease in comparatively well-weatherable plagioclase and biotite and an increase in the weathering product kaolinite (Fig. 3).

The anatase standard material was not overestimated in the Rietveld quantification, indicating that there is no significant proportion of X-ray amorphous material in the samples. Nevertheless, it cannot be excluded that background intensity is partly taken by fitted minerals, as indicated by broadened reflexes of some phases, which may lead to underestimation of the standard and thus represents a potential source of quantification uncertainty. The proportional scale and trends between the samples are, however, considered trustworthy. Topaz and F-apatite were identified as F-bearing mineral phases, while fluorite has not been detected. Stoichiometric bulk rock F contents were calculated from the Rietveld data (Fig. 3). The values plot in the range of the typical F content of San Miguelito rhyolites (Table 1). As suggested by element correlation analysis (Fig. 2c), topaz is the main F host mineral in these rocks. Nevertheless, the availability of topaz-F to be disintegrated into its surrounding environment is rather limited due to the high resistance to weathering of this mineral. This is supported by topaz content being highest in the most altered rhyolite sample (Fig. 3). In contrast, F-apatite successively decreases with increasing alteration indicating that this mineral, despite its lower abundance, may be the more important F^- source in terms of remobilization and release into groundwater. Apatite weathering is heavily temperature dependent (Guidry and Mackenzie 2000) and may be triggered under the given warm and semiarid climate of the study area, and especially under thermal water conditions. These findings also suggest

increasing degree of alteration

2 cm

	quartz	sanidine	plagioclase	kaolinite	biotite	zircon	corundum	topaz	F-apatite	stoichiometric topaz-F	stoichiometric apatite-F
(a)	25.87	25.50	34.43	1.96	6.18	0.74	2.76	1.58	1.15	0.182	0.044
(b)	26.16	31.86	29.15	2.62	5.73	0.50	1.46	1.46	1.04	0.167	0.039
(c)	27.95	31.21	25.48	5.00	4.57	0.60	1.24	2.27	0.78	0.260	0.030

Fig. 3 Microscopic images and mineralogical composition of rhyolites, and F contents calculated for identified F-bearing mineral phases (in wt.%) in samples **a**, **b** and **c** from Sierra San Miguelito (SSM)

that rhyolites of the Lower volcanic sequence are potentially effective F⁻ sources, despite their lower bulk F contents (Table 1, Fig. 2b).

Dissolved fluoride development and hydrochemistry

Figure 1 shows the region with F⁻ concentrations > 2 mg/L in extraction boreholes for 1987 and 2007 data. A comparison of these two datasets suggests that the new boreholes constructed to the NW and S of SLP City are under the influence of high F⁻ water. These boreholes are located directly on the felsic volcanic material, and they tap the regional flow without any further possible control. However, F⁻ concentrations in other parts of the city area remained similar to values reported for 1987 (Carrillo-Rivera et al. 2002).

The relation between groundwater temperature and its F⁻ concentration for 1987 and 2007 data (Fig. 4) suggests that an acceptable water quality (in terms of F⁻ < 1.5 mg/L) may be obtained by keeping the extracted raw water mixture below a temperature of ~ 30 °C. Exceptions from this approach are represented by those boreholes with groundwater extraction inducing intermediate flow water travel through the volcanic material which produces an excess in F⁻ in extracted water (data above the $R^2 = 0.8$ trendline, i.e., boreholes located in the framed fields in Fig. 4 with > 1.5 mg/L F⁻). Usage of these waters for drinking purposes requires an individual F⁻ management. Nevertheless, should other influences be absent in extraction boreholes, the control of discharge temperature at ~ 30 °C or lower may keep F⁻ concentrations within satisfactory limits.

Figure 5 indicates the relation between borehole discharge water temperature and F⁻ concentration in selected extraction boreholes, comparing 1987 and 2007 data
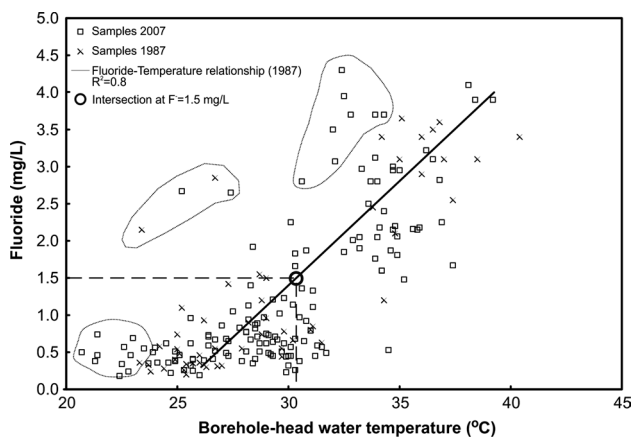
Fig. 4 Water discharge temperature versus fluoride concentration for 1987 and 2007 samples. Framed fields mark sample groups with F⁻ concentrations significantly in excess of the displayed F⁻/temperature relation
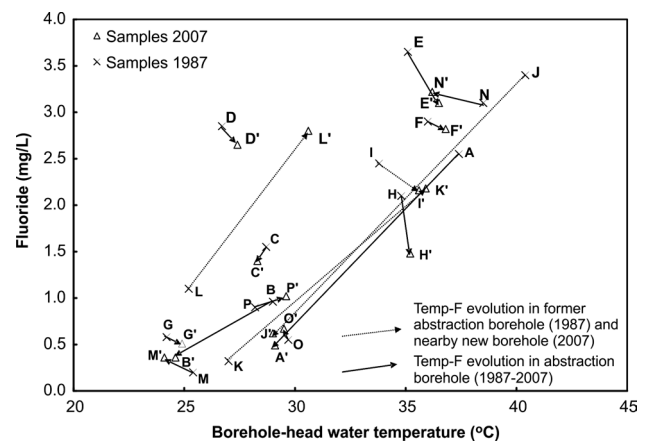
Fig. 5 Comparison of water discharge temperature versus fluoride concentration for selected boreholes for 1987 and 2007 data

(Table 2). Reduced extracted water temperature (solid line) for measurements made at boreholes A, B, and C implies that inflow water changed along the mixture path resulting in a decreased F⁻ concentration. Other boreholes show a slight decrease in F⁻ but some increase in temperature (boreholes D, E, F, G, H, and I). Groundwater relative age, i.e., residence time, in terms of Li concentration appears to be similar in most of these cases (Table 2). Lithium concentrations in groundwater are controlled by water/rock interaction processes, mainly via release of Li during silicate weathering (Négrel et al. 2012). This metal is typically associated with felsic rocks like rhyolites and pegmatites due to its incompatibility during magmatic differentiation (e.g., Benson et al. 2017). Edmunds and Smedley (2000) observed positive correlation of Li with groundwater temperature as well as with ¹⁴C age, and used the element as an indicator of groundwater residence time. It was also successfully used to discriminate between thermal and shallow groundwater (Carrillo-Rivera et al. 1996; Lambrakis et al. 2013).

New boreholes (I, J, K, L) have been constructed close to sites where old boreholes were removed due to a deteriorating extraction regime. Data for the old borehole (1987) as compared to the new site (2007) put forward that the proposed mixture line for the 1987 data (cf. Carrillo-Rivera et al. 2002) is still valid (Table 2, Fig. 5).

Figure 6 directly visualizes the impact of temperature changes on the variations of F⁻ (Fig. 6a) and Li (Fig. 6b) concentrations in groundwater, emphasizing that both parameters can be regarded as functions of groundwater temperature with $R^2 = 0.84$ for F⁻ and 0.91 for Li.

Natural F⁻ controls derived from 1987 data (Carrillo-Rivera et al. 2002) seem applicable to previous as well as new boreholes. As Li is expected to behave in a conservative manner, this property might be used to propose possible reactions relating F⁻ along the groundwater flow path to the

Table 2 Temperature and lithium and fluoride results for groundwater samples from 1987 and 2007 (T given in °C, Li and F concentrations in mg/L)

Borehole	T (1987)	T (2007)	ΔT (2007–1987)	Li (1987)	Li (2007)	ΔLi (2007–1987)	F (1987)	F (2007)	ΔF (2007–1987)
A	37.4	29.1	− 8.3	0.17	0.08	− 0.09	2.55	0.49	− 2.06
B	29.0	24.1	− 4.9	0.12	0.01	− 0.11	0.96	0.36	− 0.60
C	28.7	28.3	− 0.4	0.10	0.11	0.01	1.55	1.40	− 0.15
D	26.7	27.4	0.7	0.07	0.07	0.00	2.85	2.65	− 0.20
E	35.1	36.5	1.4	0.18	0.20	0.02	3.65	3.10	− 0.55
F	36.0	36.8	0.8	0.18	0.18	0.00	2.90	2.82	− 0.08
G	24.2	24.9	0.7	0.04	0.03	− 0.01	0.58	0.51	− 0.07
H	34.8	35.2	0.4	0.15	0.15	0.00	2.10	1.48	− 0.62
I[a]	33.8	35.6	1.8	0.17	0.17	0.00	2.45	2.16	− 0.29
J[a]	40.4	29.0	− 11.4	0.22	0.05	− 0.17	3.40	0.62	− 2.78
K[a]	27.0	35.9	8.9	0.03	0.19	0.16	0.32	2.18	1.86
L[a]	25.2	30.6	5.4	0.04	0.13	0.09	1.10	2.80	1.70
M	25.4	24.6	− 0.8	0.01	0.01	0.00	0.20	0.36	0.16
N	38.5	36.2	− 2.3	0.18	0.18	0.00	3.10	3.22	0.12
O	29.7	29.5	− 0.2	0.05	0.02	− 0.03	0.55	0.67	0.12
P	28.2	29.6	1.4	0.04	0.05	0.01	0.90	1.02	0.12

[a]New boreholes (2007 data) constructed near the old borehole sites (1987 data)
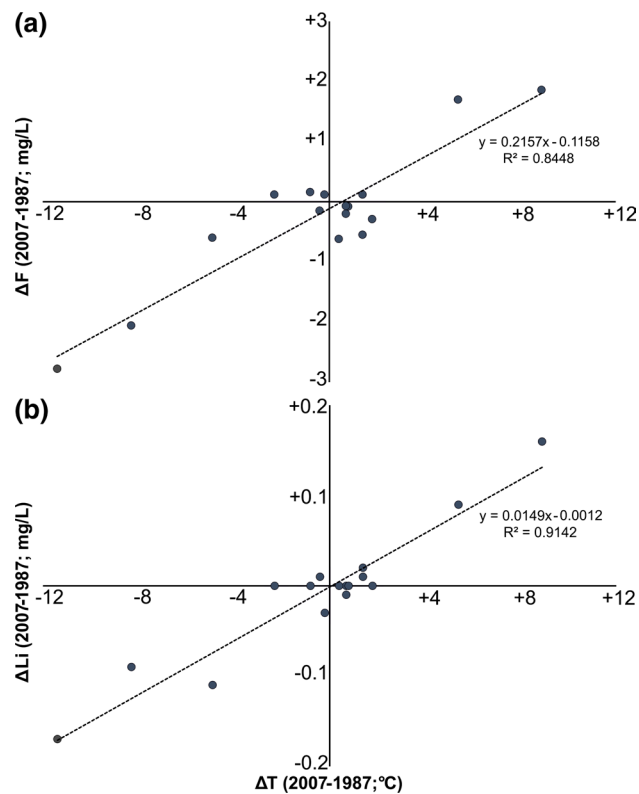
Fig. 6 Relation of groundwater temperature changes from 1987 to 2007 versus changes in F⁻ (**a**) and Li (**b**) groundwater concentrations in the same period of time
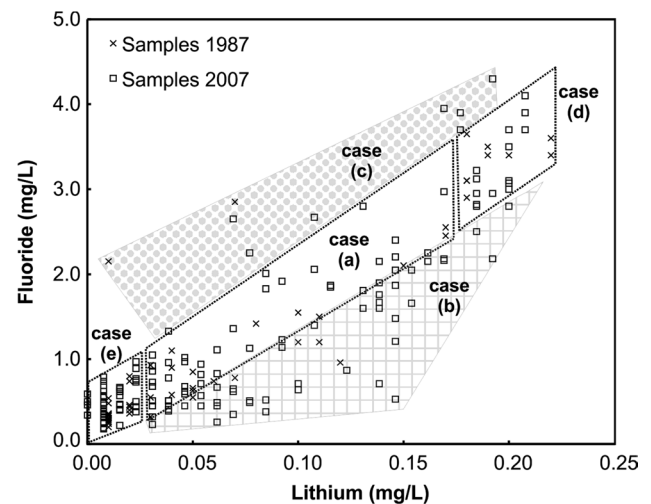
Fig. 7 Relation of Li (residence time indicator) versus F⁻ for 1987–2007 data, showing F⁻ control cases (a) by mixture, (b) reduction by precipitation, (c) F⁻ increase from sources in addition to regional flow, (d) high F⁻ source (regional flow) and (e) low F⁻ source (intermediate flow)

extraction borehole. Figure 7 is constructed with boundaries for different cases that could be anticipated based on the nature of Li as water age indicator (Edmunds and Smedley 2000) as well as with further support by the discharge temperature of the regional flow (33.8–40.4 °C), and that of intermediate flow (25.5 ± 1 °C), respectively. Assuming that the relationship between temperature values and F⁻ concentration has prevailed, from Fig. 4 and/or from the equation

relating groundwater temperature (T) to its F^- concentration [$F = (T - 25.005)/3.562$], samples depict the mixing end-members of cases (d) and (e) (Carrillo-Rivera et al. 2002). Figure 7 suggests that also more recent extraction induces water from the regional flow system, often with higher Li concentration implying longer residence time (Edmunds and Smedley 2000), and higher temperature than in the 1987 situation (*case d*).

Case a represents the mechanical mixture between thermal and cold water end-members (regional *(case d)* and intermediate *(case e)* flows). Data presented in Fig. 7 suggest that a large number of boreholes is affected by mixed waters of different Tóthian groundwater flow system origin represented by *case a*. Fluoride increase (from 1987 to 2007) of borehole K (Fig. 5) is explained by the increase in the regional flow portion in the mixture with intermediate flow. Conversely, F^- reduction in borehole J is explained by an additional input of the intermediate flow end-member with lower F^- and Li concentrations (Table 2).

Case b shows the effect of fluorite precipitation accompanied by reduced F^- concentrations in the aqueous phase, as these samples, concluding from their 1987 position, would be expected to belong to *case a* if only pure conservative mixing occurred. The solubility control by CaF_2 and associated loss of dissolved F^- in the water mixture when it travels through the Ca-rich granular material ($CaCO_3$ containing sediments in the SLP graben basin) are plausible possibilities to explain F^- reduction suggested by *case b*. Fewer samples represent *case c*; they indicate fluoride input to groundwater from other sources in addition to the regional flow end-member.

Phreeqc calculations of saturation indices (Carrillo-Rivera et al. 2002) suggest that F^- concentration in the water of the regional flow system is controlled by fluorite solubility irrespective of extraction groundwater temperature. Calculations made using geothermometry proposed that this water attains a temperature of about 75 °C at depth (at about 1000–1500 m) and that it is about in equilibrium with respect to fluorite (and calcite). Extracted groundwater (at discharge temperature) is undersaturated with respect to fluorite. Such results are interpreted as a F^- loss occurring in the ascent of regional flow water to borehole discharge. A natural F^- concentration control may be postulated by increasing calcium and lowering water temperature, which is feasible as the thermal water at borehole head is calcite undersaturated (or near equilibrium). Since fluorite oversaturation is not anticipated, the application of this solubility control is recommended for natural F^- reduction in future groundwater extraction schemes. Specific borehole design taking the geological and hydrogeological conditions into consideration may allow groundwater from the regional flow system to circulate through the Ca-rich granular material to trap dissolved F^- prior to extraction. Consequently, the application of the proposed in situ controls of F^- attenuation by the hydrogeological environment through response and traveling path of the groundwater flow systems may be favored over conventional treatment plants which would result in higher costs due to the substantial initial capital investment of such plants. Furthermore, their dimensioning and performance are unclear, and they might be inefficient due to the observed evolution in water quality with extraction time as a function of variation in the extraction rate of intermediate/regional inflow to the borehole. Dependent on the selected water treatment approach, an additional environmental and financial concern would be the management of accumulating sludge.

There is a need for a better understanding of regional flow systems by borehole drillers and borehole operators. Screens and discharge yield through step drawdown tests should be designed to tap more raw water from vertical flow, i.e., groundwater which reacted with Ca-rich aquifer sediments to precipitate F^- as CaF_2 before extraction. Raw waters with temperatures above the derived temperature control (30 °C) should be avoided or cooled down—ideally in the borehole—by appropriately controlling pumped water velocity for extra cooling time. These measures possibly come at the expense of higher capital expenditures (CapEx) but will be much cheaper than treatment of raw water for F^- removal. The latter should not be first choice due to (1) substantial operational expenditures (OpEx) adding to the CapEx, (2) the need for trained people to run the plants adapting to changing raw water composition as discussed before, and (3) the disperse water supply infrastructure which will require numerous treatment plants or a wide transport pipe network, both of which are hardly feasible.

Conclusions

Elevated F^- concentrations in groundwater around San Luis Potosí City were shown to primarily derive from geogenic mobilization of F-bearing mineral phases present in the surrounding felsic volcanic rocks. The natural F^- control mechanisms in the different Tóthian flow systems proposed in this study appear to be managing the presence and distribution of F^- in extracted groundwater in the SLP catchment. Data for 1987 and 2007 further suggest that the previously proposed counteractive measures (Carrillo-Rivera et al. 2002) *before* water is extracted are applicable and that it is advisable to fully consider them when new boreholes are constructed as well as in the management of existing ones as the efforts to remove F^- once it reaches the surface are costly and environmentally critical.

The proposed model and F^- controls could have wider applicability in similar hydrogeological frameworks in other parts of Mexico, the USA, and the world, where groundwater

derived from different Tóthian flow systems in a particular mixture is obtained for consumption in the growing number of recognized areas affected by elevated F^- concentrations.

References

Aguillón-Robles A, Aranda Gómez JJ, Solorio-Munguía JG (1994) Geología y tectónica de un conjunto de domos riolíticos del Oligoceno medio en el sur del Estado de San Luis Potosí. México. Rev Mexic Cienc Geol 11(1):29–42

Amini M, Mueller K, Abbaspour KC, Rosenberg T, Afyuni M, Møller KN, Sarr M, Johnson CA (2008) Statistical modeling of global geogenic fluoride contamination in groundwaters. Environ Sci Technol 42:3662–3668

APHA-AWWA-WPCF (1989) Standard methods for the examination of water and wastewater, vol 17. APHA-AWWA-WPCF, Washington, DC

Banning A, Rüde TR (2015) Apatite weathering as a geological driver of high uranium concentrations in groundwater. Appl Geochem 59:139–146

Benson TR, Coble MA, Rytuba JJ, Mahood GA (2017) Lithium enrichment in intracontinental rhyolite magmas leads to Li deposits in caldera basins. Nat Commun 8:270

Bjørklund G, Christophersen OA, Chirumbolo S, Selinus O, Aaseth J (2017) Recent aspects of uranium toxicology in medical geology. Environ Res 156:526–533

Cardona A (2007) Hidrogeoquímica de sistemas de flujo, regional, intermedio y local resultado del marco geológico en la Mesa Central: reacciones, procesos y contaminación. Dissertation UNAM, Mexico City

Cardona A, Carrillo-Rivera JJ (2006) Hidrogeoquímica de sistemas de flujo intermedio que circulan por sedimentos continentales derivados de rocas riolíticas. Ingeniería Hidráulica en México XXI(3):69–86

Carrillo-Rivera JJ, Cardona A, Moss D (1996) Importance of the vertical component of groundwater flow: a hydrochemical approach in the valley of San Luis Potosí, Mexico. J Hydrol 185:23–44

Carrillo-Rivera JJ, Cardona A, Edmunds WE (2002) Using extraction regime and knowledge of hydrogeological conditions to control high-fluoride concentration in obtained groundwater: San Luis Potosí basin, Mexico. J Hydrol 261:24–47

Carrillo-Rivera JJ, Varsányi I, Kovács L, Cardona A (2007) Tracing groundwater flow systems with hydrochemistry in contrasting geological environments. Water Air Soil Pollut 184:77–103

Christiansen EH, Burt DM, Sheridan MF, Wilson RT (1983) The petrogenesis of topaz rhyolites from the Western United States. Contrib Miner Petrol 83:16–30

Edmunds WM, Smedley PL (1996) Groundwater geochemistry and health: an overview. In: Appleton JD, Fuge R, McCall GJH (eds) Environmental geochemistry and health. Geological Society Special Publication, No. 113, UK, pp 91–95

Edmunds WM, Smedley PL (2000) Residence time indicators in groundwater: the East Midlands Triassic sandstone aquifer. Appl Geochem 15(6):737–752

Edmunds WM, Ahmed KM, Whitehead PG (2015) A review of arsenic and its impacts in groundwater of the

Ganges–Brahmaputra–Meghna delta, Bangladesh. Environ Sci Process Impacts 17(6):1032–1046

Fendorf S, Michael HA, Van Geen A (2010) Spatial and temporal variations of groundwater arsenic in South and Southeast Asia. Science 328(5982):1123–1127

Gaciri SJ, Davies TC (1993) The occurrence and geochemistry of fluoride in some natural waters of Kenya. J Hydrol 143:395–412

García-Pérez A, Irigoyen-Camacho ME, Borges-Yáñez A (2013) Fluorosis and dental caries in mexican schoolchildren residing in areas with different water fluoride concentrations and receiving fluoridated salt. Caries Res 47:299–308

Grimaldo M, Borja-Aburto VH, Ramírez AL, Ponce M, Rosas M, Diaz-Barriga F (1995) Endemic fluorosis in San Luis Potosí, México. Environ Res 68:25–30

Guidry MW, Mackenzie FT (2000) Apatite weathering and the Phanerozoic phosphorus cycle. Geology 28(7):631–634

Guo H, Zhang Y, Xing L, Jia Y (2012) Spatial variation in arsenic and fluoride concentrations of shallow groundwater from the town of Shahai in the Hetao basin, Inner Mongolia. Appl Geochem 27:2187–2196

Guo H, Wen D, Liu Z, Jia Y, Guo Q (2014) A review of high arsenic groundwater in Mainland and Taiwan, China: distribution, characteristics and geochemical processes. Appl Geochem 41:196–217

Guzmán EJ, De Cserna Z (1963) Tectonic history of México. Mem Am Assoc Pet Geol 2:115–120

INEGI (2013) Dirección General de Geografía. Continuo de Elevaciones Mexicano 3.0 (CEM 3.0). http://www.inegi.org.mx. Accessed 17 May 2017

Jia Y, Guo H, Jiang Y, Wu Y, Zhou Y (2014) Hydrogeochemical zonation and its implication for arsenic mobilization in deep groundwaters near alluvial fans in the Hetao Basin, Inner Mongolia. J Hydrol 518:410–420

Jia Y, Guo H, Xi B, Jiang Y, Zhang Z, Yuan R, Yi W, Xue X (2017) Sources of groundwater salinity and potential impact on arsenic mobility in the western Hetao Basin, Inner Mongolia. Sci Tot Environ 601–602:691–702

Labarthe-Hernández G, Tristán-González M, Aranda-Gómez JJ (1982) Revisión estratigráfica del Cenozoico de la parte central del Estado de San Luis Potosí. Inst Geol Met UASLP Folleto Técnico 85

Lambrakis N, Zagana E, Katsanou K (2013) Geochemical patterns and origin of alkaline thermal waters in Central Greece (Platystomo and Smokovo areas). Environ Earth Sci 69:2475–2486

Lucas J (1988) Fluorine in the natural environment. J Fluor Chem 41:1–8

McArthur JM, Sikdar PK, Hoque MA, Ghosal U (2012) Waste-water impacts on groundwater: Cl/Br ratios and implications for arsenic pollution of groundwater in the Bengal Basin and Red River Basin, Vietnam. Sci Total Environ 437(11):390–402

Medellín-Milán P, Alfaro-De la Torre MC, De Lira-Santillán AG, Nieto-Ahumada B, Sarabia-Meléndez I (1993) Fluoride in drinking water, its correlation with parameters of the aquifer and effect on dental health in the City of San Luis Potosí, México. Amer Water Works Assoc 2:1011–1024

Navarro O, González J, Júnez-Ferreira HE, Bautista C-F, Cardona A (2017) Correlation of arsenic and fluoride in the groundwater for human consumption in a semiarid region of Mexico. Procedia Eng 186:333–340

Négrel P, Millot R, Guerrot C, Petelet-Giraud E, Brenot A, Malcuit E (2012) Heterogeneities and interconnections in groundwaters: coupled B, Li and stable-isotope variations in a large aquifer system (Eocene Sand aquifer, Southwestern France). Chem Geol 296–297:83–95

Nicolli HB, Garcia JW, Falcon CM, Smedley PL (2012) Mobilization of arsenic and other trace elements of health concern in

groundwater from the Sali River Basin, Tucuman Province, Argentina. Environ Geochem Health 34:251–262

Nieto-Samaniego AF, Macías-Romo C, Alaniz-Álvarez SA (1996) Nuevas edades isotópicas de la cubierta volcánica cenozoica de la parte meridional de la Mesa Central, México. Rev Mexic Cienc Geol 13(1):117–122

Orozco-Esquivel MT, Nieto-Samaniego AF, Alaniz-Alvarez SA (2002) Origin of rhyolitic lavas in the Mesa Central, Mexico, by crustal melting related to extension. J Volcanol Geotherm Res 118:37–56

Parkhurst DL, Thorstenson DC, Plummer LN (1980) PHREEQC— a computer program for geochemical calculations. USGS-Water Resources Investigations 90-92

Raju NJ (2017) Prevalence of fluorosis in the fluoride enriched groundwater in semi-arid parts of eastern India: geochemistry and health implications. Quat Intern 443:265–278

Rodríguez-Ríos R (1997) Caractérisation du magmatisme et des minéralisations associées du dome de Pinos et des dômes de rhyolite à topaze du Champ Volcanique de San Luis Potosí (Mexique). Dissertation, Université Henri Poincaré, Nancy

Sarabia MFI (1989) Contenido de fluoruros en el agua de consumo y sus efectos en el tejido dental, San Luis Potosí, México. M.Sc. Thesis, Universidad Autónoma de San Luis Potosí

Stecher O (1998) Fluorine geochemistry in volcanic rock series: examples from Iceland and Jan Mayen. Geochim Cosmochim Acta 62(18):3117–3130

Stretta EJP, Del Arenal R (1960) Estudio para el abastecimiento del agua potable para la ciudad de San Luis Potosí. Instituto de Ciencia Aplicada UNAM, México

Tóth J (1998) Groundwater as a geological agent: an overview of the causes, processes, and manifestations. Hydrogeol J 7:1–14

Tristán-González M (1986) Estratigrafía y tectónica del Graben de Villa de Reyes, en los estados de San Luis Potosí y Guanajuato, México. Inst Geol UASLP, Folleto Técnico 10

Tristán-González M, Labarthe-Hernández G, Aguillón-Robles A, Torres-Hernández JR, Aguirre-Díaz G (2006) Diques piroclásticos en fallas de extensión alimentadores de ignimbritas en el occidente del Campo Volcánico del Río Santa María, S.L.P (resumen). GEOS 26(1):163

Tristán-González M, Aguillón-Robles A, Barboza-Gudiño JR, Torres-Hernández JR, Bellon H, López-Doncel RA, Rodríguez-Ríos R, Labarthe-Hernández G (2009) Geocronología y distribución espacial del Campo Volcánico de San Luis Potosí. Bol Soc Geol Mex 61(3):287–303

Valenzuela-Vásquez L, Ramírez-Hernández J, Reyes-López J, Sol-Uribe A, Lázaro-Mancilla O (2006) The origin of fluoride in groundwater supply to Hermosillo City, Sonora, México. Environ Geol 51:17–27